Evaluation of MSNDs for Fast-Neutron Detection and the TREAT Hodoscope

Priyarshini Ghosh, Wenkai Fu, Ryan Fronk, Douglas S. McGregor, Jeremy A. Roberts

Department of Mechanical and Nuclear Engineering
Kansas State University
pghosh@ksu.edu, wenkaifu@ksu.edu, rfronk@ksu.edu, mcgregor@ksu.edu, jaroberts@ksu.edu

INTRODUCTION

The need for next-generation, accident-tolerant fuels has generated significant interest in the restart of domestic fuels testing at the Transient REActor Test (TREAT) facility. A key feature of the TREAT reactor core is an open, horizontal channel that allows line-of-sight viewing of test specimens using various instrumentation during steady-state and transient operation [1]. This instrumentation includes the hodoscope, which consists of over 300 steel-collimated channels coupled to Hornyak buttons (and other detectors) for detection of fast neutrons emitted from fission of the test specimen [1]. Posterior analysis can be used to reconstruct fuel motion and other properties from the collimated channel signals [2].

A large-scale effort is underway to develop next-generation instrumentation for transient testing at TREAT (and, potentially, other facilities). Work at KSU specifically aims to provide improved detection systems for hodoscope applications. It was initially proposed to adapt KSU-developed Microstructured Semiconductor Neutron Detectors (MSNDs [3]) for use as fast-neutron detectors. The current generation of MSNDs is designed for thermal-neutron detection based on ^{6}Li and can achieve intrinsic efficiencies nearing 30% owing to the large (n,t) cross section of ^{6}Li and clever optimization of the geometry.

In order to evaluate MSNDs for fast-neutron detection, two approaches were considered: (1) use of a hydrogenous material to thermalize neutrons to exploit the intrinsic efficiencies of current MSNDs, and (2) substitution of a fast-sensitive reactant for ^{6}Li. The former approach is attractive because it makes use of proven, off-the-shelf technology and leads to reasonable time resolution and efficiency. Unfortunately, use of thermalization leads to prohibitive degradation of spatial resolution. The second approach will require further experimental efforts, but scoping analyses suggest ^{235}U- or ^{237}Th-loaded MSNDs may achieve sufficient efficiencies. The rest of this summary examines these issues in more detail.

APPROACH 1 – THERMALIZATION

Modeling and Analysis

To assess use of thermal-sensitive MSNDs, a simple, 7-channel mock-up was designed to represent a portion of a hodoscope, shown in Fig. 1. The depth (along the z-axis) is 7.62 cm. A single MSND is modeled in each of the detector channels surrounded by high-density polyethylene (HDPE); a detailed channel schematic is shown in Fig. 2. The green region is composed of 5% borated polyethylene (BPE). Both HDPE and BPE are efficient at moderating fast neutrons. In addition, the boron content in BPE is a good thermal-neutron absorber, and may prevent cross-talk, i.e., neutrons entering the target channel diffusing to other channels and being detected. It is important to minimize such cross-talk to provide accurate, spatial mapping of the fuel motion.

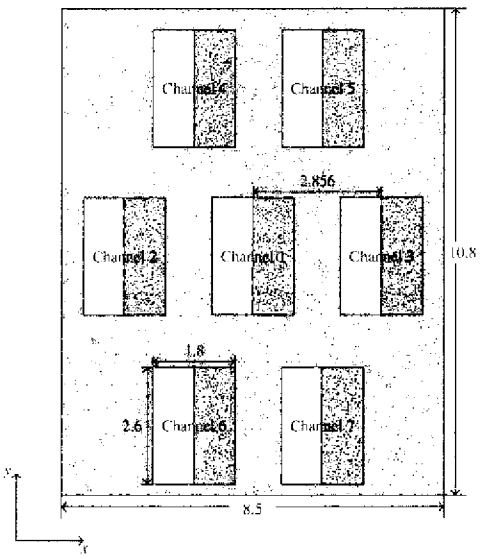

Fig. 1: Overall schematic. White regions are detector channels filled with HDPE, green regions represent 5% BPE, and gray regions are MSNDs. Channel 1 is recognized as the target channel with the source located at its center in the xy plane. All values shown are in cm.

Models of the designed mock-up and the MSND were developed in MCNP6[4]. Two sources were modeled. The first was an isotropic point source of ^{252}Cf, which is available as a source for experimental validation, placed at the center of the target channel. The second was a mono-directional planar source directed along the z axis, corresponding to collimated neutrons, with a thermal ^{235}U fission spectrum; Fig. 2 shows the planar source location and dimensions. All calculations were performed using ENDF/B-VII.0 data[5].

Because the majority of the fission neutrons coming out of the collimators are beyond the thermal range, and the Li-based MSND is thermal-sensitive, it is interesting to investigate the relationship between the neutron flux and the time in the target channel. The simulated results are shown in Fig. 3, for which the cell-averaged flux in the target channel completely filled with HDPE was computed the for mono-directional source. The uncertainties of these and all other numerical results to be shown are less than 1% and not included. The results show that for times from 2×10^{-6} s to 2×10^{-5} s, the flux is primarily thermal (energy < 1eV), with the thermal flux exceeding the non-thermal flux by more than an order of

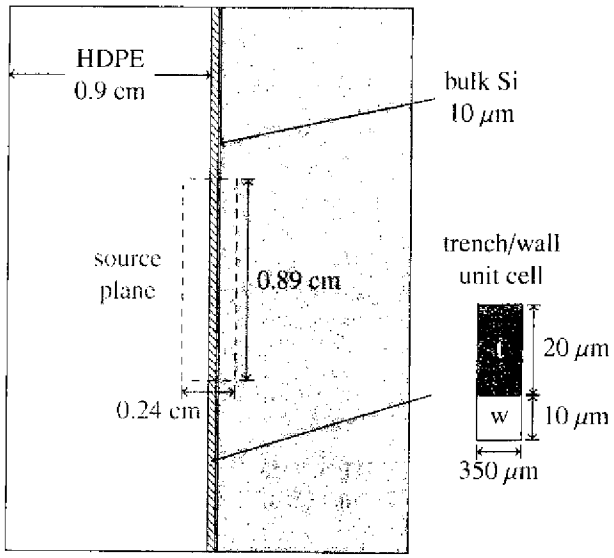

Fig. 2: Schematic for target channel with HDPE and thermal-sensitive MSND (xy-plane shown).

magnitude. Although thermalization introduces delays on the order of 1 μs, the net temporal resolution should be adequate for hodoscope applications.

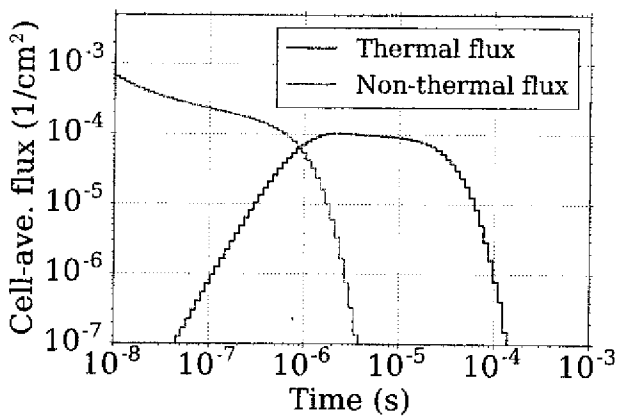

Fig. 3: MCNP results of the neutron flux in the target channel varying with time.

In order to estimate the detection efficiency in the mockup, a sequence of MSNDs was placed into the target channel along the z axis. Again, the mono-directional neutron source was used. The pulses generated from the sensitive areas in the MSND models were summed using the F8 tally, and the results are shown in Fig. 4. The detection efficiency is observed to saturate at about 0.8% when more than 7 MSNDs were used, which can be explained by the fact that the neutron flux will decrease with increased distance from the source. Best-case efficiencies for Hornyak buttons as used at TREAT appear to be approximately 0.2% for fission-spectrum neutrons [6], while modern variants (e.g., Eljen Technology's EJ-410) may have efficiencies closer to 0.7%.[1] Hence, an array of MSND's might yield an improved intrinsic efficiency over previous devices.

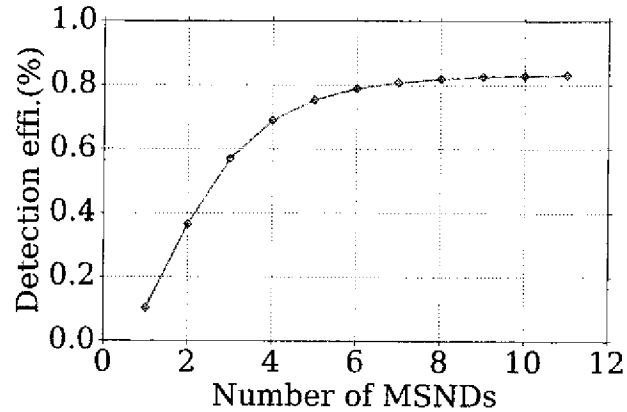

Fig. 4: Simulated detection efficiency as a function of the number of MSNDs used.

The major purpose of TREAT is to measure the fuel motion inside the test sample, and this objective requires a minimum cross-talk. To evaluate cross-talk quantitatively, the cross-talk ratio (CTR) is defined as

$$\text{CTR} = \frac{\text{number of pulses in neighbor channel}}{\text{number of pulses in target channel}}, \quad (1)$$

The calculated CTRs in each channel for the two source cases are shown in TABLE I and discussed in relation to the experimental results below.

Experimental Validation

To validate the computational results, count rates at different channels from neutrons emitted from a ^{252}Cf source, which was placed at the center of channel 1 in xy plane, were recorded, and the experimental setup is shown in Fig. 5.

The experimental results, as shown in TABLE I, confirm the existence of significant cross-talk, with the measured cross-talk (all over 60%) being substantially larger than the MCNP model predictions by 10-30% in each channel. A large portion of this difference may be due to neutron scattering not included in the model. Specifically, the walls, floor, ceiling, equipment, and table on which the mock-up was situated, along with any other, nearby hydrogenous objects may have caused neutron-scattering and lead to a higher count rate [7]. However, because both the predicted and measured results were underwhelming, no further work was performed to reduce the discrepancies.

APPROACH 2 – FAST-SENSITIVE REACTANTS

Current generations of MSNDs have geometries optimized for the collection of charged ^{3}H and ^{4}He emitted from neutron interactions with ^{6}Li. Fast sensitive reactants like ^{235}U (assuming thermal-neutron filtration) or ^{237}Np undergo fission to produce two, massive ions that have smaller ranges by at least a factor of two. Unfortunately, manufacturing processes

[1] In this case, a report intrinsic efficiency of 0.7% may translate to a lower efficiency for the particular application of interest.

Channel number	1	2	3	4	5	6	7
Average count rate (counts/min)	185.7±4.31	128.95±3.58	128.35±3.58	114.75±3.38	113.65±3.37	114.5±3.38	115.15±3.39
Measured CTR (%), isotropic source		69.44	69.11	61.79	61.20	61.66	62.01
Calculated CTR (%), isotropic source		50.12	70.80	34.95	50.47	36.22	53.42
Calculated CTR (%), mono-direc. source		13.36	16.52	7.53	10.49	7.64	10.77

TABLE I: A comparison between the measured and the calculated CTRs in different channels.

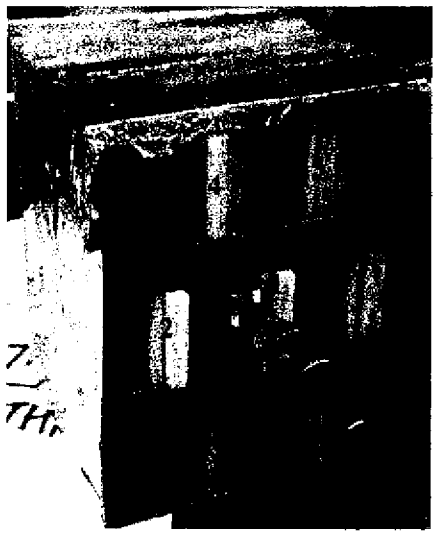

Fig. 5: Experimental setup: a MSND was inserted to each channel to measure the corresponding count rate.

limit the size of trenches to roughly the sizes used in current MSNDs, thereby limiting the potential intrinsic efficiency.

Modeling and Analysis

To understand the potential intrinsic efficiency, a study was performed for both ^{232}Th, ^{235}U, ^{238}U, and ^{237}Np. Pairs of MSNDs were modeled with adjacent trench faces centered in a single channel. All moderating material was omitted. The MSND dimensions used are consistent with those shown in Fig. 2. In other words, the devices modeled are very similar to off-the-shelf devices with substituted reactants.

Modeling was performed using MCNP6 in two parts. First, the total fission rate in the reactant (per source particle) was computed. Second, the number of fission fragments (born uniformly and emitted isotropically in the reactant) depositing sufficiently large energy (above 350 keV) in the bulk-Si diode was computed per fission fragment emitted. Shown in Fig. 6 is the predicted number of fissions per source particle, as a function of the number of MSNDs (oriented pair-wise along the collimator path), for all 4 reactants at a density of 8 g/cm^3. As in the previous results, all relative uncertainties are below 1% and not shown.

For simplicity, two representative fission fragments (^{90}Sr and ^{137}Cs with initial energies of 112 and 74 MeV) were used to estimate the number of counts per fission fragment emitted. Fig. 7 shows this ratio as a function of trench width for three wall thicknesses and a trench depth of 350 μm for ^{235}U (the results for other reactants are nearly equivalent). These results

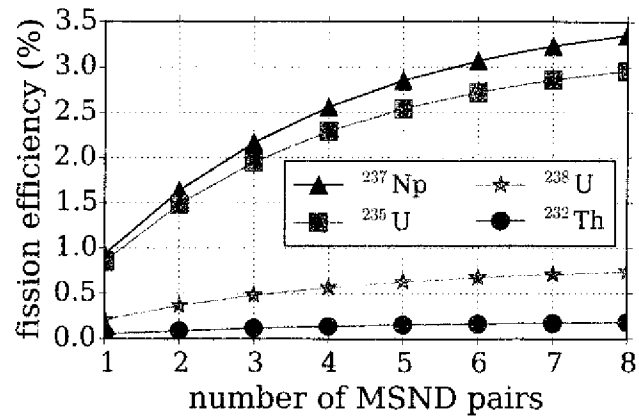

Fig. 6: Expected number of fissions in all MSNDs per source particle

indicate that the wall thickness does not impact the efficiency significantly, consistent with the fact that fission fragments need only traverse a short wall distance to deposit sufficient energy for production of a countable pulse. Contrarily, the trench width impacts efficiency greatly because large trenches lead to excessive self-absorption.

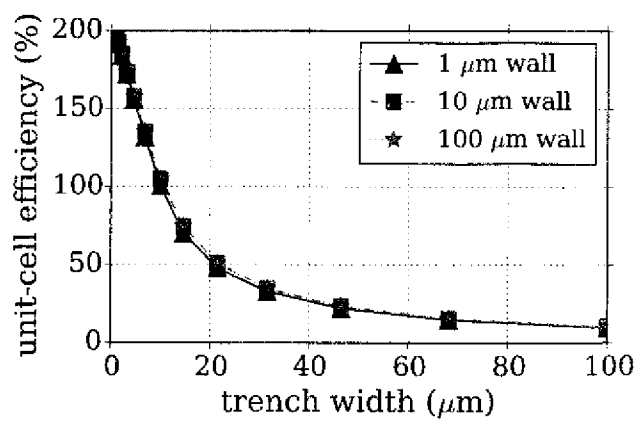

Fig. 7: Expected number of counts per fission in trench-wall unit cell.

With a trench width of 20 μm (the same as was modeled for the thermal-sensitive MSNDs), the intrinsic efficiency of 6 MSNDs is, therefore, approximately 2% $\times$ 50% $\approx$ 1.0% for ^{235}U with slight improvements if ^{237}Np were used (with much lower efficiency for ^{232}Th and ^{238}U). Hence, this fast-sensitive array has a higher predicted efficiency than an equivalent, thermalized approach. Cross-talk is expected to be much

lower than for the thermalized case, but analysis remains for future work. Although some cross-talk is expected for ^{235}U, the threshold nature of the ^{232}Th, ^{238}U, and ^{237}Np fission cross sections should virtually eliminate the issue.

Experimental Work

Initial work has been performed to deposit uranium into MSND trenches. Uranium was precipitated from a uranyl nitrate solution based on a previously-formulated recipe at KSU[8]. The original particles from the uranyl nitrate precipitate had widths ranging from 30-160 μm.

An attempt was made to reduce the particle size to fit inside the 20-μm trenches using homogeneous precipitation from solution by hydrolysis of urea at elevated temperatures. Such precipitation yields novel, ammonia-intercalated alpha-type hydroxide phases and exhibits a much milder concentration gradient than mechanically adding NH_4OH, resulting in precipitation products of higher purity, smaller particles, and less agglomeration. Homogeneous precipitation of uranyl nitrate was carried out in a pressure cooker at 120°C for 30 minutes. Significant reduction in particle width was observed, with widths of 6-17 μm.

The MSND was fixed in place to the bottom of a centrifuge tube and the solution was poured over it. The tube was centrifuged for an hour. Scanning Electron Microscopy (SEM) imaging showed that the accumulation of the particles at the entrance caused the major portion of the trenches to remain empty, as shown in Fig. 8. The few particles that were able to enter the trench agglomerated together into bigger clumps at the bottom of the column. X-ray fluorescence and X-ray diffraction studies indicated that a negligible amount of uranium entered the trenches, which suggests that uranyl nitrate is unsuitable for this application.

Fig. 8: SEM image of under-filled MSND trench.

CONCLUSIONS

Ongoing work at KSU to develop hodoscope-detector alternatives based on MSNDs has been presented. Although thermal-sensitive MSNDs lead to reasonable efficiency, the thermalization used degrades spatial resolution by too much. Analysis performed suggests that fast-sensitive MSND's may be possible through use of ^{235}U or ^{237}Np, but there remain several engineering challenges to overcome before demonstration. A possible approach for using ^{235}U (or other actinides) may be to use high-energy planetary ball-milling of oxides to achieve sub-micron sizes for eventual deposition in MSND trenches. Simultaneous efforts are also being made at KSU to investigate the use of alternative devices, including novel improvements to the materials and geometry of Hornyak-button variants.

ACKNOWLEDGMENTS

This material is based upon work supported by the U.S. Department of Energy, Office of Nuclear Energy under Award Number DE-NE0008305.

REFERENCES

1. A. DE VOLPI, R. PECINA, R. DALY, D. TRAVIS, R. STEWART, and E. RHODES, "Fast-neutron hodoscope at TREAT: development and operation," *Nuclear Technology*, **27**, *3*, 449–487 (1975).
2. T. H. BAUER, A. E. WRIGHT, W. R. ROBINSON, J. W. HOLLAND, and E. A. RHODES, "Behavior of modern metallic fuel in treat transient overpower tests," *Nuclear technology*, **92**, *3*, 325–352 (1990).
3. S. L. BELLINGER, R. G. FRONK, T. J. SOBERING, and D. S. MCGREGOR, "High-efficiency microstructured semiconductor neutron detectors that are arrayed, dual-integrated, and stacked," *Applied Radiation and Isotopes*, **70**, *7*, 1121–1124 (2012).
4. T. GOORLEY, M. JAMES, T. BOOTH, F. BROWN, J. BULL, L. COX, J. DURKEE, J. ELSON, M. FENSIN, R. FORSTER, ET AL., "Initial MCNP6 release overview," *Nuclear Technology*, **180**, *3*, 298–315 (2012).
5. M. CHADWICK, P. OBLOŽINSKÝ, M. HERMAN, N. GREENE, R. MCKNIGHT, D. SMITH, P. YOUNG, R. MACFARLANE, G. HALE, S. FRANKLE, ET AL., "ENDF/B-VII. 0: next generation evaluated nuclear data library for nuclear science and technology," *Nuclear data sheets*, **107**, *12*, 2931–3060 (2006).
6. C. FINK, "Optimization of a Hornyak-button Detector for Fast-neutron Detection," *IEEE Transactions on Nuclear Science*, **29**, *1*, 718–721 (1982).
7. R. FRONK, S. BELLINGER, L. HENSON, D. HUDDLESTON, T. OCHS, T. SOBERING, and D. MCGREGOR, "High-efficiency microstructured semiconductor neutron detectors for direct 3He replacement," *Nuclear Instruments and Methods in Physics Research A*, **779**, 25–32 (2015).
8. M. REICHENBERGER, T. ITO, P. UGOROWSKI, B. MONTAG, S. STEVENSON, D. NICHOLS, and D. MCGREGOR, "Electrodeposition of uranium and thorium onto small platinum electrodes," *Nuclear Instruments and Methods in Physics Research A*, **812**, 12–16 (2016).